Poultry Science

Mitochondrial dysfunction and calcium dyshomeostasis in the pectoralis major muscle of broiler chickens with wooden breast myopathy

Xinrui Zhang,* Tong Xing,* Jiaolong Li,† Lin Zhang,* and Feng Gao*,[1]

*College of Animal Science and Technology, Key Laboratory of Animal Origin Food Production and Safety Guarantee of Jiangsu Province, Jiangsu Collaborative Innovation Center of Meat Production and Processing, Quality and Safety Control, Nanjing Agricultural University, Nanjing 210095, PR China; and †Institute of Agri-Products Processing, Jiangsu Academy of Agricultural Sciences, Nanjing 210014, PR China

ABSTRACT The incidence of wooden breast (**WB**) meat of commercial broiler chicken has been increasing in recent years. Histological examination found that the occurrence of WB myopathy was accompanied by the pectoralis major (**PM**) muscle damage. So far, the potential mechanisms are not fully understood. This study aimed to explore the underlying mechanism of the damage of WB-affected PM muscle caused by changes in mitochondrial function, mitochondrial redox status and Ca^{2+} homeostasis. A total of 80 market-age Arbor Acres male broiler chickens were sampled and categorized into control (**CON**) and WB groups based on the evaluation of myopathic lesions. PM muscle samples were collected ($n = 8$ in each group) for histopathological evaluation and biochemical analyses. Ultrastructural examination and histopathological changes suggested the occurrence of PM muscle damage in broiler chickens with WB myopathy. The WB group showed an increased level of reactive oxygen species and enhanced antioxidant capacities in mitochondria of PM muscle. These changes were related to impaired mitochondria morphology and mitochondrial dysfunction. In addition, abnormal expressions of Ca^{2+} channels led to substantial Ca^{2+} loss in SR and cytoplasmic Ca^{2+} overload, as well as Ca^{2+} accumulation in mitochondria, resulting in Ca^{2+} dyshomeostasis in PM muscle of broiler chickens with WB myopathy. Combined, these findings indicate that WB myopathy is related to mitochondrial dysfunction, mitochondrial redox status imbalance and Ca^{2+} dyshomeostasis, leading to WB-affected PM muscle damage.

Key words: wooden breast, broiler chicken, mitochondrial function, mitochondrial redox status, Ca^{2+} homeostasis

2023 Poultry Science 102:102872
https://doi.org/10.1016/j.psj.2023.102872

INTRODUCTION

In recent years, the genetic selection of modern commercial broilers has developed in the direction of high breast muscle yield and fast growth rate to meet the growing global demand for poultry meat (Petracci et al., 2015). However, the significant increase of broiler chicken production efficiency has been accompanied by the occurrence of wooden breast (**WB**) and other myopathies. WB myopathy attracts the attention of researchers and poultry practitioners owing to its high incidence and adverse effects on meat quality (Petracci et al., 2019). The macroscopic characteristics of WB myopathy are hardened areas, as well as the appearance of turbid viscous coating of the outer surface, white striping, and small hemorrhages in the pectoralis major (**PM**) muscle (Sihvo et al., 2014). The poor appearance not only reduces the purchase desire of consumers, but also damages nutritional value and quality of chicken meat, causing serious economic losses to the poultry industry.

The pathogenesis of WB myopathy is very complex, and the etiology of WB myopathy has been studied from multiple perspectives in recent years. Petracci et al. (2015) suggested that genetic selection of both high breast muscle yield and growth rate were highly correlated with the occurrence of WB myopathy. Xing et al. (2021) reported that birds with WB myopathy had higher PM muscle yield. Accumulating evidence suggests that muscle fiber hypertrophy caused by excessive breast muscle development reduces perimysial and endomysial available space available for capillaries and leads to hypoxia, which may cause oxidative stress and Ca^{2+} dyshomeostasis (Petracci et al., 2019; Velleman, 2019). Oxidative stress and Ca^{2+} dyshomeostasis are key factors leading to skeletal muscle damage, which affects skeletal muscle development and structure (Michelucci et al., 2021; Lian et al., 2022). Velleman et al. (2018) found that WB myopathy detrimentally affected the sarcomere organization in a broiler line-specific manner,

Received February 8, 2023.
Accepted June 9, 2023.

[1]Corresponding author: gaofeng0629@sina.com

and the disorganization of the sarcomere structure led to the dysfunction of the PM muscle as well as the reduction of meat quality. Xing et al. (2021) also reported increased activity of lactate dehydrogenase in plasma of WB-affected birds, which indicated severe muscle damage. Therefore, the assessment of the potential mechanism causing WB-affected PM muscle damage might be favor to an in-depth understanding of etiology.

Growing evidence suggests that oxidative stress and change of redox homeostasis may be biological processes related to the pathogenesis of WB myopathy (Mutryn et al., 2015; Abasht et al., 2016). Oxidative stress denotes the increase in the level of intracellular reactive oxygen species (**ROS**) (Lee et al., 2021). In tissues under oxidative stress, the ratio of ROS to antioxidants is highly imbalanced, and long-term cellular damage can occur (Hubert and Athrey, 2020). Zhao et al. (2018) observed that administration of As_2O_3 and $CuSO_4$ triggered oxidative stress of skeletal muscle by increasing the level of hydroxy radical, hence causing an adverse effect on the histomorphology and redox status of the PM muscle. Hasegawa et al. (2022) reported that when the levels of ROS in muscle fibers were increased, mitochondrial homeostasis was not maintained and the damage levels increase in various membranes of the cell, leading to the disruption of normal physiological functions in WB-affected PM muscle. Mitochondria of skeletal muscle are the key source of ROS, as well as the major target of oxidative damage and the vital intracellular redox buffering system (Lee et al., 2021). Mitochondria function deeply relies on the morphology and ultrastructure (Ignatieva et al., 2021). Disruption of the electrons flux in mitochondrial membrane structure, as well as the respiratory chain promoted oxidation reactions through electron leakage and the posterior formation of phospholipid hydroperoxides (de Oliveira et al., 2017). Hubert and Athrey (2020) expressed that it was necessary to characterize the mitochondrial structure related to WB. Pan et al. (2021) observed mitochondria swelling and cristae dissolution in PM muscle of WB-affected birds, indicating that mitochondrial architecture was seriously damaged. Hosotani et al. (2020) reported that the altered mitochondrial clearance and the accumulation of damaged mitochondria underlay the severe pathological features of WB. Studies have shown that mitochondrial architecture damage is associated with mitochondrial dysfunction, which is manifested by the mitochondrial membrane potential (**$\Delta\Psi$m**) dissipation, electron transport chain (**ETC**) damage, redox status imbalance and inhibition of ATP synthesize (Indo et al., 2007; Boengler et al., 2017). Integrated metabolomic and RNA-seq analyses by Wang et al. (2023) also showed that mitochondrial dysfunction was presented in WB. Excessive ROS generation due to mitochondrial dysfunction can cause oxidative stress, leading to the damage of muscle and dysfunction in muscular disease (Michelucci et al., 2021). However, research concerning mitochondrial function changes in WB-affected birds is limited.

Ca^{2+} is an important intracellular messenger, controlling various cellular functions (Dong et al., 2006). Zambonelli et al. (2016) found an up-regulated amount of Ca^{2+} in WB fillets. Mutryn et al. (2015) hypothesized that intracellular Ca^{2+} overload may impact sarcolemmal membrane integrity in the PM muscle of WB chicken. The loss of Ca^{2+} homeostasis, often in the form of cytoplasmic increase of Ca^{2+}, leads to muscle disorganization and damage (Dong et al., 2006). Intracellular Ca^{2+} homeostasis is intricately regulated by various types of Ca^{2+} channels and important Ca^{2+} stores including sarcoplasmic reticulum (**SR**) and mitochondria (Maklad et al., 2019). Oxidative stress can lead to the dysregulation of the Ca^{2+} channels and subsequent cytoplasmic Ca^{2+} overload by disrupting intracellular Ca^{2+} homeostasis, resulting in myofiber degeneration, myofibrillar disarray, sarcolemmal rupture, structural alterations, and mitochondrial damage (Michelucci et al., 2021). The long-term effect of the cytoplasmic Ca^{2+} overload could be the initiation of a "vicious cycle" of mitochondrial Ca^{2+} overload that causes mitochondrial dysfunction, which promotes ROS generation and oxidative stress, as well as aggravates cell damage and finally results in mitochondria-mediated cell death (Ermak and Davies, 2002). In addition, excessive Ca^{2+} may activate intracellular lipases or proteases and lead to an increase in Ca^{2+} influx and muscle fiber breakdown, initiating a "vicious cycle" of Ca^{2+} release and muscle damage (Oberc and Engel, 1977). Whereas the regulation of transmembrane Ca^{2+} channels and intracellular Ca^{2+} stores on Ca^{2+} homeostasis in PM muscle of WB-affected broiler chickens has not been reported.

So far, limited data exist on the mechanism of the damage of WB-affected PM muscle. Hence, this study aimed to systemically compare the histological, mitochondrial function, mitochondrial redox status, and Ca^{2+} homeostasis in PM muscle of normal and WB myopathic broiler chickens to clarify the underlying mechanisms mediating the damage of PM muscle.

MATERIALS AND METHODS

Experimental Broiler Chickens Selection and Sample Collection

Bird managements and all experimental procedures were approved by Nanjing Agricultural University Institutional Animal Care and Use Committee under protocol number SYXK 2021-0014. Arbor Acres males broiler chickens raised in layered cages and received commercial diets and husbandry routines were used in this study. Water and feed were offered ad libitum to birds. A total of 80 broilers aged 42 d were clinically examined for WB myopathy involving visual observations for posture, wing contact, and bilateral manual palpation for hardness of the PM muscle in a cranio-caudal direction based on the methods proposed by Papah et al. (2017). Then, 12 suspected WB-unaffected and 12 WB-affected live birds were chosen, stunned electrically (50 V, alternating current, 400 Hz for 5 s each) and slaughtered via exsanguination immediately. After slaughter, broilers were necropsied relying on the standard reported by

Papah et al. (2017), 8 WB-unaffected fillets (no detectable increase in firmness of the breast area) and 8 WB fillets (moderately firm in a focally extensive area or markedly firm exhibiting diffuse coverage of the breast area) by palpation of the PM muscle were selected by 3 trained personnel eventually. Samples from the superficial layer of the cranial part of the left PM muscle were collected and fixed in 2.5% glutaraldehyde or 4% paraformaldehyde for ultrastructural or histological evaluation observation. The remaining PM muscle tissues were frozen in liquid nitrogen and stored at −80°C for the subsequent biochemical assessments.

Histopathological Evaluation

At room temperature, PM muscle samples were fixed in paraformaldehyde (4%) over 24 h for histological analysis. After fixing the samples transversely, dehydration was performed by using ethanol. Sequentially, the samples were embedded in paraffin, cut into slices (8-μm) and placed on slides. Paraffin must be removed from sections with dimethyl-benzene before staining. And then the slides were incubated in ethanol solution before hydrated. Finally, trichromatic staining of hematoxylin and eosin (**H&E**) was performed according to the procedures described by Xing et al. (2017). Under identical conditions, myopathic lesions of each slide were assessed with same magnification by a light microscope (Axio Scope. A1, Carl Zeiss, Oberbochen, Germany). Normal breast and WB with typical characteristics were ensured by the examination of the microscopic structure. Histological evaluations were performed by the method of Clark and Velleman (2016).

Ultrastructural Observation

Glutaraldehyde solution (2.5%) was used to fix the PM muscle samples overnight at 4°C. After washing with PBS, samples was postfixed with osmium tetroxide (1%). The tissues were dehydrated by using ethanol after washing with PBS again. Then the samples were embedded in Spurr's resin. An ultra-microtome (RMC Power Tome XL, Leica, Wetzlar, Germany) was used to section the samples. Subsequently, 30 nm ultrathin sections were collected and stained with 3% uranyl acetate and lead citrate. Finally, a transmission electron microscope (TEM, Hitachi H-7650, Tokyo, Japan) was used to examine the ultrastructural changes.

Mitochondrial Isolation and Mitochondrial Function Assay

PM muscle mitochondria were isolated by using a commercial kit (Beyotime Biotechnology, Shanghai, China) as the manufacturer's instructions. The mitochondrial suspension was stored at −80°C. A BCA kit (Beyotime, Shanghai, China) was used to determine protein concentration of mitochondrial suspension.

The corresponding commercial kits (Sangon Biotech Co. Ltd., Shanghai, China) were used to detect the activities of mitochondrial electron transport chain complex I and III as the manufacturer' s instructions. A JC-1 kit (Solarbio Science & Technology, Co. Ltd., Beijing, China) was used to perform the mitochondria membrane potential ($\Delta\psi$m) assay. In short, JC-1 dyeing working solution (180 μL) was mixed with mitochondrial suspension (20 μL) for 10 min. Finally, a microplate reader was used to measure the fluorescence intensity. The monomeric and aggregated forms of JC-1 were detected with the wavelengths of 485 (excitation) and 620 nm (emission). The mitochondrial swelling was assessed referring to the method of Xing et al. (2021).

Sarcoplasmic Reticulum Isolation

SR extraction refers to the method of Zhang et al. (2011). The total of 2 g PM muscle samples with 5 mL ice-cold extract (pH = 7.4, 0.1 M KCl, 20 mM Mops, and 0.1 mM EDTA) were homogenized twice at 13,500 rpm for 15 s each time. Then homogenate was centrifuged at 4°C for 20 min at 5,000 *g*, and the supernatant was retained in a centrifuge tube while the precipitate was added to ice-cold extract again for repeated extraction. Twice supernatant was combined and centrifuged at 4°C for 10 min at 12,000 *g*. The supernatant was filtered with a filter membrane (0.45 μm) and a final concentration of 0.6 M KCl was prepared by adding KCl solution. After that, the samples were incubated at 4°C for 20 min, then centrifuged at 4°C for 1 h at 23,500 *g*. Next, the precipitate was suspended in buffer solution (pH = 7.0, 0.3M sucrose and 20 mM Mops) and incubated for 1h, and then centrifuged at 4°C for 1 h at 40,000 *g*, the precipitate was SR. Finally, the SR precipitate was suspended in the buffer solution again to form SR suspension and stored at −80°C. The BCA kit was used to detect protein concentration of SR suspension.

Analysis of Reactive Oxygen Species and Malondialdehyde of Mitochondrial and SR

As the manufacturer's instructions, the ROS levels and the content of malondialdehyde (**MDA**) in collected mitochondria and SR suspensions were detected by using the corresponding commercial kits (Nanjing Jiancheng Bioengineering Institute, Nanjing, China).

Analysis of Mitochondrial Antioxidant Capacity

The redox state of the obtained mitochondrial suspension was assessed. The content of glutathione (**GSH**), and the activities of glutathione reductase (**GR**), glutathione peroxidase (**GSH-Px**), copper−zinc superoxide dismutase (**Cu-ZnSOD**), manganese superoxide dismutase (**MnSOD**), and total superoxide dismutase (**T-SOD**) were detected using the corresponding commercial kits bought from Nanjing Jiancheng Bioengineering

Institute (Nanjing, China). GR was denoted in units per g protein, the other results were denoted in units per milligram protein.

Determination of Ca^{2+} Concentration in Cytoplasm, Mitochondria, and SR of PM Muscle

Referring to the method of Wang et al. (2019), 2 g PM muscle sample was weighed and homogenized in an ice-cold 0.15 M KCL solution. The homogenizing conditions were 12,000 rpm for 2 times and each time for 1 min. Afterward, the homogenate was centrifuged at 4°C for 10 min at 27,000 *g* and the PM muscle tissue supernatant was collected for the Ca^{2+} concentration. Trichloroacetic acid (5%) was added to the supernatant of PM muscle and the suspensions of mitochondria and sarcoplasmic reticulum, and then strontium chloride (0.5%) was added after standing for 10 min. At room temperature, the samples were centrifuged at 10,000 *g* for 10 min. The supernatant of PM muscle tissue, mitochondrial, and SR was collected, and then the Inductively Coupled Plasma (iCAP, 7000, SERIES, Thermo Fisher Scientific, Waltham, MA) was used to detect the Ca^{2+} concentration.

RNA Purification and Real-Time Quantitative PCR Analysis

RNAiso plus reagent (Takara Biotechnology Co., Ltd., Dalian, China) was used to isolate total mRNA from PM muscles. The mRNA was reversely transcribed into cDNA using a cDNA synthesis commercial kit (Takara Biotechnology Co. Ltd.). SYBR Premix Ex Tap (Vazyme Biotechnology Co., Ltd., Nanjing, China) was used for quantitative real-time quantitative polymerase chain reaction (qPCR) on an ABI PRISM 7500 (Applied Biosystems, Foster City, CA). Table S1 shows the primer sequences used for qPCR. The $2^{-\Delta\Delta Ct}$ method with Tubulin as the internal reference gene was used to calculate the relative mRNA.

Total Protein Extraction and Western Blot Analysis

RIPA lysis buffer (Beyotime Biotechnology, Jiangsu, China), which containing phosphatase and protease inhibitors, was added into frozen PM muscle samples and then homogenized. The homogenate was centrifuged at 4°C for 20 min at 12,000 *g*, and the supernatant was collected. The BCA kit was used to detect the protein concentration. Equal amounts of total protein were electrophoresed on SDS-PAGE (6% or 10%) and transferred to a polyvinylidene fluoride membrane (Millipore, Billerica, MA). At room temperature, bovine serum albumin (5%) was used to block the membranes for 1.5 h. Next, the membranes were incubated in primary antibodies against PMCA1, NCX1, TRPC1 (Zen-Bioscience, Chengdu, China), MCU (Abclonal, Wuhan, China), SERCA1 (Abcam, Cambridge, UK), IP3R (ProteinTech, Wuhan, China), and Tubulin (Beyotime, Shanghai, China) overnight at 4° C with gentle shaking. Finally, at room temperature, the membranes were incubated by using the corresponding secondary antibodies (Cell Signaling Technology, Danvers, MA) for 1 h. The protein bands were treated with an ECL chemiluminescence detection kit (Vazyme Biotechnology Co., Ltd.) and then visualized with the ChemiDoc TM Imaging System (BIO-RAD, Singapore). Quantity One software (Bio-Rad) was used to quantify the density of bands and the relative protein expression was calculated by ImageJ software with Tubulin as a normalized control.

Statistical Analysis

SPSS Statistics (SPSS, Inc., Chicago, IL) was used for data analysis and Student's *t*-tests was used to compare the differences between individuals. Data were reported as means ± SE. A trend was considered at $0.05 < P < 0.1$, and significance was indicated at $P \leq 0.05$.

RESULTS

Histological Observation of PM Muscle

The ultrastructure of PM myofibers was observed by using the TEM. The CON myofibers were oriented longitudinally and the comprising sarcomeres arranged in register with each other, and exhibited typical architecture of the normal skeletal muscles. However, the WB-affected myofibers showed disturbance of Z-lines exhibited by irregular and disconnected of Z-lines. In addition, we also found separation and dissolution of myofibrils (Figure 1A).

As shown in Figure 1B, the muscle fibers were closely arranged with a polygonal shape and had no myodegenerative fibers in the CON group. On the contrary, the WB group showed polyphasic myodegeneration with regeneration, and muscle fibers were loosely arranged. Variably sized muscle fibers were rounded and separated or replaced by a loose or more organized connective tissue with inflammatory cell infiltration.

Wooden Breast Myopathy Induced PM Muscle Mitochondria Morphology Changes and Mitochondrial Dysfunction

As shown in Figure 2A, the morphology of mitochondria in the CON group showed intact membrane integrity, well-defined matrix and cristae. On the contrary, mitochondria in the WB group exhibited membrane swelling, dissolution, and collapse of cristae, as well as dissolution of the matrix to some extent.

Moreover, the activities of mitochondrial respiratory chain complex I and III, as well as the $\Delta\Psi m$ were significantly reduced in the WB compared to the CON ($P < 0.05$; Figures 2B and 2C). Meanwhile, the OD values at 540 nm in the WB were lower than the CON, indicating that the mitochondria were prone to swelling in the WB-affected PM muscle ($P < 0.05$; Figure 2D).

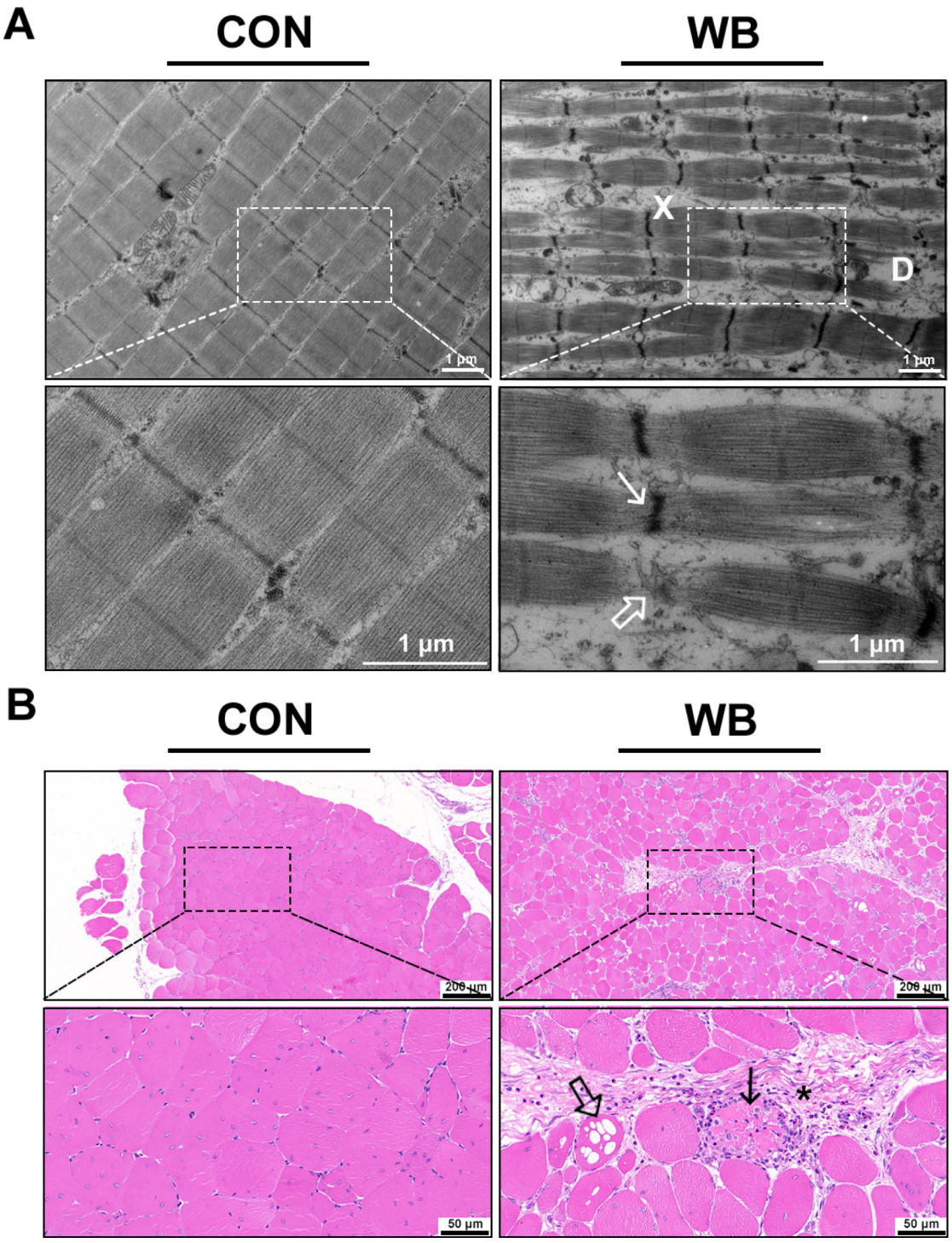

Figure 1. Histopathological observation and results of muscle fiber average diameter in pectoralis major muscle of CON and WB birds. (A) Representative transmission electron microscope images of PM muscle. WB-affected PM muscles exhibit irregular (arrow) and disconnected (open arrow) Z-lines, dissolution (D) and separation of myofibrils (X). (B) Representative images of hematoxylin and eosin staining of PM muscle. Degenerating fibers (arrow) are often surrounded by inflammatory cell infiltration and abundant collagen-rich connective tissue (asterisk); vacuolar degeneration (open arrow).

Redox Status in Mitochondria and mRNA Expression of Mitochondrial Antioxidant Factor

As exhibited in Table 1, the ROS level ($P < 0.01$) and MDA content ($P < 0.05$) in mitochondria of WB-affected PM muscle were higher than the CON group. The PM muscle from WB broiler chickens showed significantly higher ($P < 0.05$) activities of GSH-Px, GR, T-SOD, MnSOD, and Cu-ZnSOD, as well as the content of GSH than the CON group. Moreover, the mRNA expressions of *GPx, GCLc GCLm, MnSOD, CuZnSOD, Trx2, TrxR2,* and *Prx3* of the WB group were up-regulated compared to the CON group ($P < 0.05$; Figures 4A−4C).

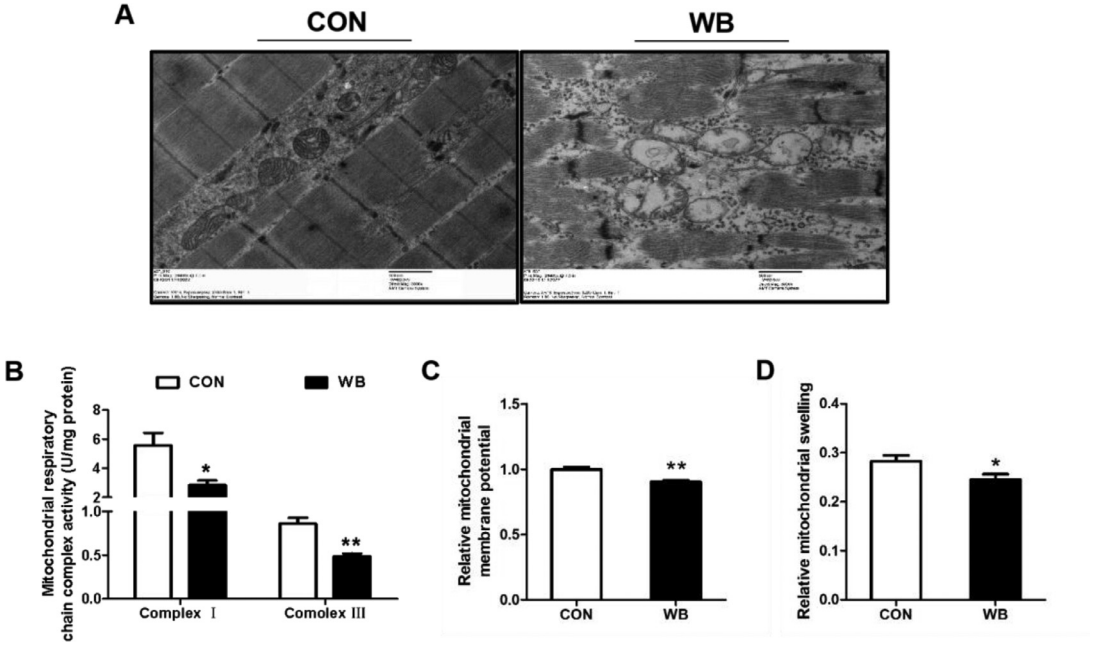

Figure 2. Mitochondria morphology and mitochondrial function changes in pectoralis major muscle of CON and WB birds. (A) Mitochondrial morphology of PM muscle. (B) Activity of mitochondrial respiratory chain complexes I and III. (C) Relative mitochondrial membrane potential. (D) Relative mitochondrial swelling. Data are expressed as the mean ± SE ($n = 8$). $^{**}P < 0.01$ and $^{*}P < 0.05$.

ROS Level and MDA Content in SR as Well as Ca^{2+} Concentration in Cytoplasm, Mitochondria and SR

The levels of ROS ($P < 0.01$) and MDA ($P < 0.05$) in SR of WB-affect PM muscle were significantly higher compared to the CON. Moreover, the Ca^{2+} concentration in SR cytoplasm was down-regulated, whereas the Ca^{2+} concentration in cytoplasm and mitochondria was up-regulated in the WB compared to the CON ($P < 0.01$).

Expression of Calcium Channels on the Membrane of SR, Cell, and Mitochondria

The mRNA expressions of *IP_3R* and *RyR1* were upregulated, whereas *SERCA1* was downregulated in the WB compared to the CON ($P < 0.05$; Figure 3A). Consistently, the protein content of IP3R and SERCA1 respectively increased and decreased in the WB compared to the CON ($P < 0.05$; Figures 5B and 5C). The mRNA expressions of *TRPC1, Oria1* and *PMCA* ($P < 0.05$; Figure 5D), as well as the protein contents of PMCA1 and TRPC1 were upregulated in the WB compared to the CON ($P < 0.01$; Figures 5E and 5F). Furthermore, WB broiler chickens exhibited significantly up-regulated mRNA expression and protein content of MCU in the PM muscle compared to the CON birds ($P < 0.01$, Figures 4G–4I).

DISCUSSION

Skeletal muscle consists of myofibers, and its main functional unit is myofibril. Sarcomere structure is significant to the livability of bird to keep the contractile ability (Velleman et al., 1997). We observed that the WB-affected muscle exhibited separation and dissolution of myofibrils, as well as disruption of Z-bands. Papah et al. (2017) found disconnected, irregular, and a loss of Z bands in WB-affected muscles of birds at 6 wk of age, suggesting that the ultrastructure of the skeletal muscle was damaged. In addition, histological studies showed that WB myopathy was accompanied by muscle damage, exhibiting obvious necrosis and myofiber degeneration, as well as the infiltration of inflammatory cell and deposition of connective tissue (Sihvo et al., 2014). This phenomenon was observed in our H&E staining of WB samples. Although we did not make statistics on muscle fiber diameter, some small-diameter muscle fibers could be observed in WB-affected PM muscle, which was consistent with previous studies (Velleman and Clark, 2015; Clark and Velleman, 2016; Xing et al., 2021). Clark and Velleman (2016) reported that the percentage of small fibers (diameter < 10 μm) was increased in WB-affected PM muscle compared to unaffected muscle. As discussed in Clark and Velleman (2016), the smaller diameter fibers are likely fibers undergoing the regeneration process to repair the damaged muscle fibers and produce new fibers. However, the repair and regeneration of muscle fibers after damage cannot fully restore the morphology and structure in the WB-affected PM muscle.

As the main site of cellular aerobic respiration, mitochondria are essential for various cellular biological processes such as stabilizing signal transduction, maintaining cellular physiological processes and ROS generation (Kotiadis et al., 2014). Myopathy associated with ultrastructural disruption of myofibers is frequently accompanied by alterations of mitochondrial structure

Table 1. Mitochondrial oxidative products and antioxidant capacity in breast muscle of broilers with normal (CON) and wooden breast (WB) pectoralis major muscle ($n = 8$).

Items	Treatments		SEM
	CON	WB	
ROS generation	1.00	1.54**	0.11
MDA (nmol/mg protein)	2.20	3.59*	0.41
GSH (umol/g protein)	9.49	12.30*	0.88
GSH-Px (U/mg protein)	16.37	21.49*	1.39
GR (U/g protein)	8.27	14.78*	1.68
T-SOD (U/mg protein)	22.54	27.43*	1.22
CuZnSOD (U/mg protein)	11.63	13.89*	0.67
MnSOD (U/mg protein)	10.91	13.54*	0.80

Abbreviations: Cu-ZnSOD, Cu−Zn superoxide dismutase; GR, glutathione reductase; GSH, glutathione; GSH-Px, glutathione peroxidase; MDA, malondialdehyde; MnSOD, manganese superoxide dismutase; ROS, reactive oxygen species; SEM, standard error of means; T-SOD, total superoxide dismutase.

*$P < 0.05$.

**Significant difference at $P < 0.01$.

(Polak et al., 2009). Similarly, in this study, the observed mitochondrial structure changes included the collapse of cristae, and dissolution of the matrix or the entire mitochondria, which was similar to the findings of Papah et al. (2017). The integrity of mitochondrial architecture determines its function, and mitochondrial dysfunction is a simultaneous consequence, as well as a contributor to skeletal muscle pathologies (Ignatieva et al., 2021). Because the tissues and organs with the highest bioenergetic requirements are also those that are primarily affected in the common metabolic and degenerative diseases, it follows that mitochondrial dysfunction may be a major contributor to complex diseases (Wallace and Chalkia, 2013). Wang et al. (2023) expressed that WB was associated with alterations in energy metabolism and mitochondrial functionality. Skeletal muscle is susceptible to mitochondrial dysfunction (Qualls et al., 2021). According to our results, the mitochondria of WB-affected PM muscle exhibited a loss of $\Delta\Psi$m and were prone to go through swelling, suggesting mitochondrial dysfunction. Hasegawa et al. (2022) also found that mitochondria were swollen in severe wooden breast cases. Furthermore, in the ETC of the inner mitochondrial membrane, complexes I and III are generally considered the main contributors to mitochondrial ROS production (Tang et al., 2014). We observed that the activities of complexes I and III were decreased significantly in the WB group. Inhibition of the mitochondrial ETC induces mitochondrial ROS overproduction and causes muscle structural damage (Indo et al., 2007; Michelucci et al., 2021). Overall, these results suggested that mitochondrial dysfunction might be an important reason for muscle damage of WB-affected broiler.

Oxidative stress and alteration of redox status may be biological processes correlated with the pathogenesis of WB myopathy (Abasht et al., 2016). Skeletal muscles are rich in mitochondria, which are crucial to intracellular redox metabolism as they produce ROS by oxidative

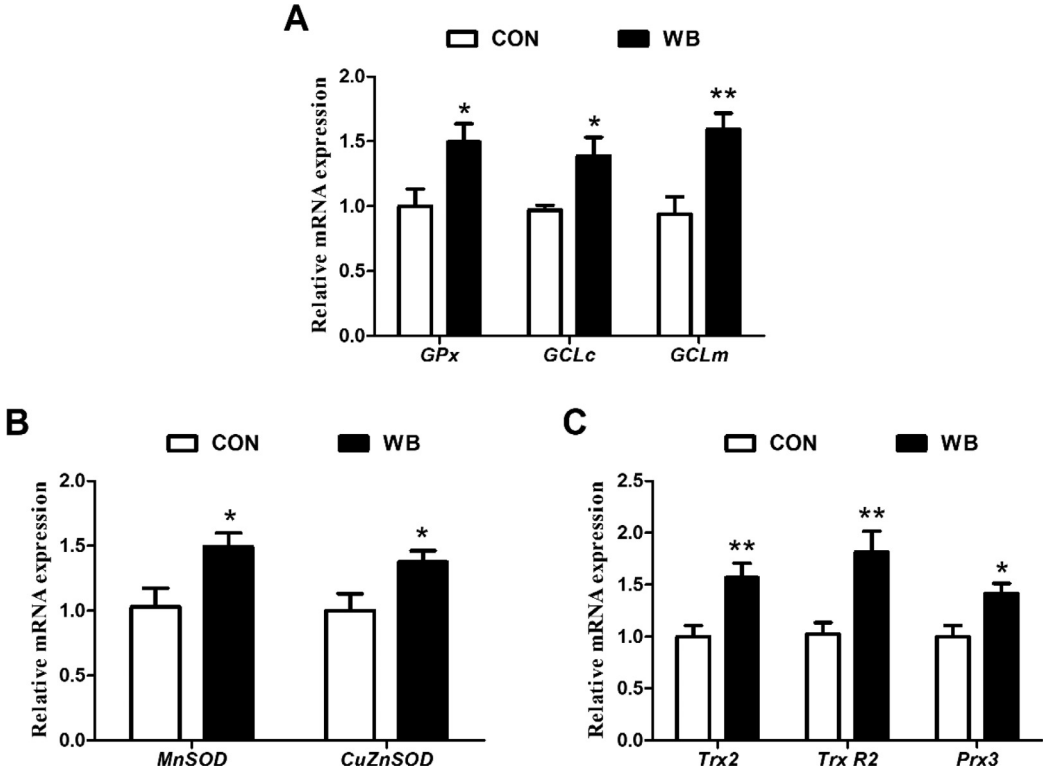

Figure 3. Relative mRNA expression of genes related to mitochondrial antioxidant factor in pectoralis major muscles of CON and WB birds. (A) Relative mRNA expression of glutathione peroxidase (GPx), glutamate-cysteine ligase catalytic (GCLc), glutamate-cysteine ligase modifier subunit gene (GCLm); (B) Relative mRNA expression of manganese superoxide dismutase (*MnSOD*), copper−zinc superoxide dismutase (Cu-ZnSOD); (C) Relative mRNA expression of thioredoxin 2 (Trx2), thioredoxin reductase 2 (Trx R2), peroxiredoxin 3 (Prx3). Data are expressed as the mean ± SE ($n = 8$). **$P < 0.01$ and * $P < 0.05$.

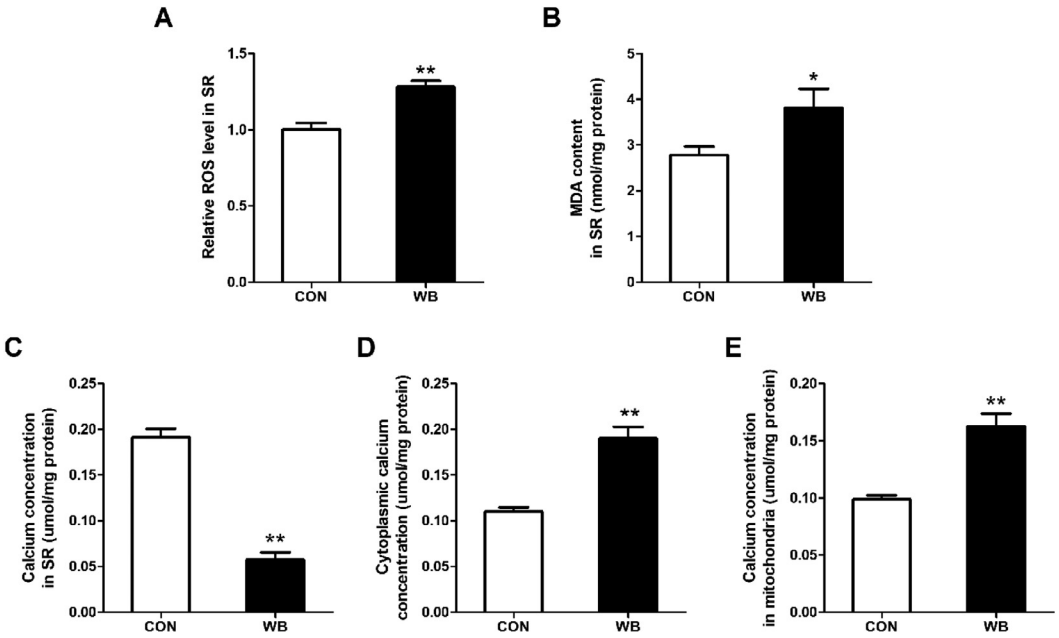

Figure 4. ROS level and MDA content in SR as well as calcium concentration in SR, cytoplasm and mitochondria in pectoralis major muscles of CON and WB birds. (A) Reactive oxygen species (ROS) level in SR. (B) Malondialdehyde (MDA) content in SR. (C) Calcium concentration in SR. (D) Calcium concentration in cytoplasm. (E) Calcium concentration in mitochondria. Data are expressed as the mean ± SE ($n = 8$). $^{**}P < 0.01$ and $^{*}P < 0.05$.

phosphorylation (Lee et al., 2021). Cytomembrane and mitochondrial membranes are mainly composed of lipids and proteins, which are vulnerable to ROS attack. MDA is the end product of lipid peroxidation, and a biomarker of oxidative stress (Lee et al., 2021). Herein, we found an excessive formation of ROS and an increase of MDA level in mitochondria of WB-affected PM muscle. ROS overproduction causes oxidative stress and cell damage by affecting membrane structure, protein function, and lipid metabolism (Lian et al., 2022). In addition, ROS overproduction even affects muscle repair and regeneration after injury, thus disturbing the function and homeostasis of skeletal muscle (Lian et al., 2022). Mitochondria possess an extensive antioxidant defense to counteract oxidative stress and maintain redox homeostasis (Lee et al., 2021). In this study, WB myopathy significantly enhanced the antioxidant enzyme activities of SODs, GSH-Px and GR, as well as the content of GSH in mitochondria of WB compared with CON. Similarly, Pan et al. (2021) indicated that WB myopathy improved the activities of T-SOD and GSH-Px in the PM muscle of broilers. However, Salles et al. (2019) found that GSH-Px activity was inhibited in the PM muscle of severe white striping birds. Xing et al. (2021) noted that the activation of antioxidant defense system depended on the stage and severity of damage or disease. Furthermore, the rate-limiting step in the endogenous GSH biosynthesis pathway is catalyzed by glutamate cysteine ligase (**GCL**), which is composed of a catalytic subunit GCLc and a modulatory subunit GCLm (Zheng et al., 2007). In addition to the SODs and GSH system, the thioredoxin (**Trx**) system, which is composed of Trx and thioredoxin reductase (**TrxR**), is also a key mitochondrial antioxidant defense system. Trx system removes ROS with a fast reaction rate by providing the electrons to peroxiredoxin (Lu and Holmgren, 2014). Liao et al. (2022) found that acute stress enhanced mitochondrial antioxidant defense system to protect the body from oxidative damage by increasing the expressions of key factors involved in Trx system and GSH system. Consistently, we found that the mRNA expressions of *GPx, GCL, MnSOD*, and *CuZnSOD*, as well as key factors involved in *Trx* system were up-regulated in the WB group, which was in line with the results of the antioxidant enzymes, confirming that WB myopathy alleviative the oxidative status by activating antioxidative genes. Pan et al. (2021) speculated that the activation of antioxidative genes related to the maintenance of the balance between antioxidants and oxidants in WB-affected PM muscle. Collectively, above results indicated the appearance of oxidative stress in mitochondria of WB-affected PM muscle as confirmed by mitochondria damage and the disturbed redox homeostasis, which possibly contributed to PM muscle damage.

Ca^{2+} controls a diverse range of cellular processes, such as muscle excitation and contraction, gene transcription, as well as cell growth and proliferation (Bootman et al., 2001). An abnormal change of the intracellular Ca^{2+} concentration causes various muscle diseases (Berchtold et al., 2000). RNA sequencing suggests that increased intracellular Ca^{2+} levels are a key feature of WB myopathy (Mutryn et al., 2015). SR is the main dynamic Ca^{2+} store compartment of the cell and is very sensitive to intracellular redox changes (Morad et al., 2000). SR provides a unique oxidative environment that promotes the formation of protein disulfide bond, which in turn leads to ROS formation in SR (Sevier and Kaiser, 2008). Under stress stimulation, SR is vulnerable to ROS attack. Our result showed that the ROS level and MDA content were increased in SR of

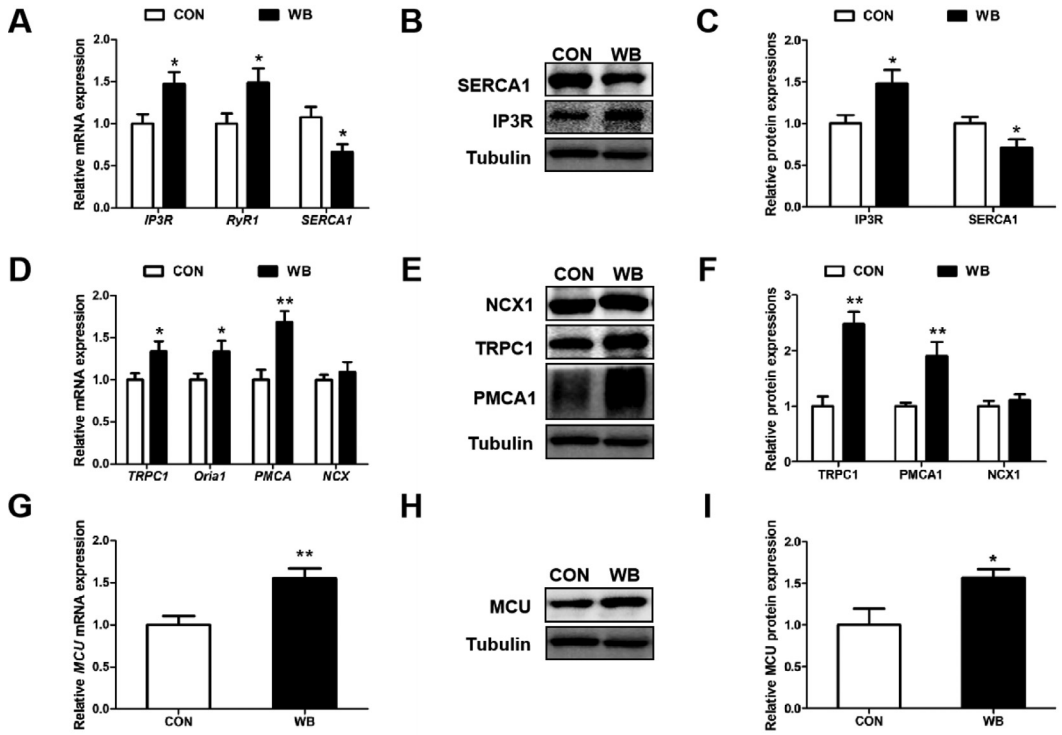

Figure 5. Calcium channel related genes and proteins expressions on the cell membrane, cell membrane and mitochondria in pectoralis major muscles of CON and WB birds. (A) Relative mRNA expressions of Inositol 1, 4, 5-trisphosphate receptor (IP3R), ryanodine receptor 1 (RyR1) and sarcoplasmic reticulum calcium-ATPase 1 (SERCA1). (B) Representative Western blotting images of SERCA1 and IP3R. (C) Relative protein expressions of SERCA1 and IP3R. (D) Relative mRNA expressions of transient receptor potential channel 1 (TRPC1), *Orai1*, plasma membrane Ca^{2+} -ATPasea (PMCA) and sodium calcium exchange (NCX). (E) Representative Western blotting images of TRPC1, PMCA1, and NCX1. (F) Relative protein expressions of TRPC1, PMCA1, and NCX1. (G) Relative mRNA expression of mitochondrial uniporter (MCU). (H) Representative Western blotting image of MCU. (I) Relative protein expression of MCU. Data are expressed as the mean ± SE for mRNA expressions ($n = 8$) and protein expressions ($n = 6$). ** $P < 0.01$ and * $P < 0.05$.

WB-affected PM muscle. Welter et al. (2022) noted a compromised structure of SR in the PM muscle WB myopathic bird, as evidenced by the alterations of the phospholipid membrane composition and increased lipid catabolism. These results suggested that excessive ROS in SR caused the oxidative damage of WB SR. Inositol 1,4,5-trisphosphate receptors (**IP3Rs**) and ryanodine receptors (**RyRs**) on SR membrane are the major Ca^{2+} release channels that release Ca^{2+} from SR into the cytoplasma, which is recovered by sarco endoplasmic reticulum Ca^{2+}-ATPase (**SERCA**) (Maklad et al., 2019). RyR/IP3R contain multiple reduced active thiols, and thiol oxidation of RyR/IP3R by ROS in general enhances channel activity and thereby promotes Ca^{2+} efflux (Bogeski and Niemeyer, 2014). However, SERCA exhibits marked dysfunction when suffers oxidative modification, which reduces Ca^{2+} influx (Strosova et al., 2011). The WB group showed the expressions of IP_3R and RyR1 increased, whereas SERCA1 decreased, which might be due to the oxidative modification caused by the increase of ROS level. Our results suggested that WB myopathy might cause the oxidative damage of SR and change the expressions of Ca^{2+} channels on the SR membrane, leading to the depletion of the SR Ca^{2+} store and a subsequent rise of cytoplasmic Ca^{2+} level. Furthermore, both transient receptor potential channel 1 (**TRPC1**) and Orai1 proteins on the cell membrane have been proposed to form Ca^{2+}-selective, store-operated calcium entry (**SOCE**) channels, which is a ubiquitous Ca^{2+} entry pathway (Ambudkar et al., 2017). Oxidative stress-induced activation of the IP3Rs and decrease of SERCA expression or activity might lead to the depletion of SR stores, facilitating SOCE activation (Taylor and Machaca, 2019; Liu et al., 2020). Our results indicated the mRNA expressions of *TRPC1* and *Orai1* as well as the protein content of TRPC1 were upregulated in WB compared with CON, which further aggravated the increase of cytoplasmic Ca^{2+} concentration in WB-affected PM muscle. Plasma membrane Ca^{2+} -ATPase (**PMCA**) is also located on the cell membrane and excretes Ca^{2+} from cytoplasm to extracellular matrix (Maklad et al., 2019). PMCA is a high-affinity Ca^{2+} clearance channel to prevent cell death induced by cytotoxic Ca^{2+} overload, and PMCA overexpression or maintenance of PMCA activity is generally accepted as being cytoprotective (Bruce, 2018). Moreover, mitochondria uptake Ca^{2+} when cytoplasmic Ca^{2+} levels increase via the mitochondrial uniporter (**MCU**) (Maklad et al., 2019). This study indicated that WB-affected PM muscle relieved cytoplasmic Ca^{2+} overload by improving the expressions of PMCA and MCU. However, the opening of MCU ultimately leads to mitochondrial Ca^{2+} overload, which promotes excessive production of ROS and initiates a "vicious cycle" of Ca^{2+}

release and muscle damage (Ermak and Davies, 2002; Michelucci et al., 2021). Overall, WB myopathy caused the oxidative stress of SR, and led to the disorder of Ca^{2+} entry and exit into extracellular matrix and intracellular organelles by dysregulating the expression of Ca^{2+} channels on cell membrane, as well as the membrane of mitochondria and SR.

CONCLUSIONS

In summary, this study provided the evidence of PM muscle damage of WB-affected birds as observed by the impaired muscle morphology and ultrastructure. Excessive ROS accumulation in mitochondria of WB muscle triggered by the mitochondrial dysfunction may be associated with oxidative stress and disturbed redox status. Additionally, oxidative damage of SR, as well as Ca^{2+} loss in SR and excessive Ca^{2+} accumulation of both cytoplasmic and mitochondrial by the abnormal expression of Ca^{2+} channels indicated the Ca^{2+} dyshomeostasis in WB-affected PM muscle. The findings indicate that WB myopathy is related to mitochondrial dysfunction, mitochondrial redox status imbalance and Ca^{2+} dyshomeostasis, leading to WB-affected PM muscle damage.

ACKNOWLEDGMENTS

This study was supported by the National Natural Science Foundation of China (32072780), and the Earmarked Fund for Jiangsu Agricultural Industry Technology System (JATS[2023]).

DISCLOSURES

The authors declare that they have no known competing financial interests or personal relationships that could have appeared to influence the work reported in this paper.

SUPPLEMENTARY MATERIALS

Supplementary material associated with this article can be found in the online version at doi:10.1016/j.psj.2023.102872.

REFERENCES

Abasht, B., M. Mutryn, R. Michalek, and L. William. 2016. Oxidative stress and metabolic perturbations in wooden breast disorder in chickens. PLoS One 11:e153750.

Ambudkar, I. S., L. B. de Souza, and H. L. Ong. 2017. TRPC1, Orai1, and STIM1 in SOCE: friends in tight spaces. Cell Calcium 63:33–39.

Berchtold, M. W., H. Brinkmeier, and M. Müntener. 2000. Calcium ion in skeletal muscle: its crucial role for muscle function, plasticity, and disease. Physiol. Rev. 80:1215–1265.

Boengler, K., M. Kosiol, M. Mayr, R. Schulz, and S. Rohrbach. 2017. Mitochondria and ageing: role in heart, skeletal muscle and adipose tissue. J. Cachexia Sarcopenia Muscle 8:349–369.

Bogeski, I., and B. A. Niemeyer. 2014. Redox regulation of ion channels. Antioxid. Redox Signal. 21:859–862.

Bootman, M. D., T. J. Collins, C. M. Peppiatt, L. S. Prothero, L. MacKenzie, P. De Smet, M. Travers, S. C. Tovey, J. T. Seo, M. J. Berridge, F. Ciccolini, and P. Lipp. 2001. Calcium signalling −an overview. Semin. Cell. Dev. Biol. 1:3–10.

Bruce, J. I. E. 2018. Metabolic regulation of the PMCA: role in cell death and survival. Cell Calcium 69:28–36.

Clark, D. L., and S. G. Velleman. 2016. Spatial influence on breast muscle morphological structure, myofiber size, and gene expression associated with the wooden breast myopathy in broilers. Poult. Sci. 95:2930–2945.

de Oliveira, M. R., S. F. Nabavi, S. M. Nabavi, and F. R. Jardim. 2017. Omega-3 polyunsaturated fatty acids and mitochondria, back to the future. Trends Food Sci. Tech. 67:76–92.

Dong, Z., P. Saikumar, J. M. Weinberg, and M. A. Venkatachalam. 2006. Calcium in cell injury and death. Annu. Rev. Pathol. 1:405–434.

Ermak, G., and K. J. Davies. 2002. Calcium and oxidative stress: from cell signaling to cell death. Mol. Immunol. 38:713–721.

Hasegawa, Y., M. Hosotani, M. Saito, T. Nagasawa, Y. Mori, T. Kawasaki, M. Yamada, N. Maeda, T. Watanabe, and T. Iwasaki. 2022. Mitochondrial characteristics of chicken breast muscle affected by wooden breast. Comp. Biochem. Physiol. A. Mol. Integr. Physiol. 273:111296.

Hosotani, M., T. Kawasaki, Y. Hasegawa, Y. Wakasa, M. Hoshino, N. Takahashi, H. Ueda, T. Takaya, T. Iwasaki, and T. Watanabe. 2020. Physiological and pathological mitochondrial clearance is related to pectoralis major muscle pathogenesis in broilers with wooden breast syndrome. Front. Physiol. 11:579.

Hubert, S. M., and G. Athrey. 2020. Energy metabolism and sources of oxidative stress in wooden breast: a review. F1000Res 9:319.

Ignatieva, E., N. Smolina, A. Kostareva, and R. Dmitrieva. 2021. Skeletal muscle mitochondria dysfunction in genetic neuromuscular disorders with cardiac phenotype. Int. J. Mol. Sci. 22:7349.

Indo, H. P., M. Davidson, H. H. Yen, S. Suenaga, K. Tomita, T. Nishii, M. Higuchi, Y. Koga, T. Ozawa, and H. J. Majima. 2007. Evidence of ROS generation by mitochondria in cells with impaired electron transport chain and mitochondrial DNA damage. Mitochondrion 7:106–118.

Kotiadis, V. N., M. R. Duchen, and L. D. Osellame. 2014. Mitochondrial quality control and communications with the nucleus are important in maintaining mitochondrial function and cell health. Biochim. Biophys. Acta 1840:1254–1265.

Lee, Y. M., W. He, and Y. C. Liou. 2021. The redox language in neurodegenerative diseases: oxidative post-translational modifications by hydrogen peroxide. Cell. Death Dis. 12:58.

Lian, D., M. M. Chen, H. Wu, S. Deng, and X. Hu. 2022. The role of oxidative stress in skeletal muscle myogenesis and muscle disease. Antioxidants (Basel) 11:755.

Liao, H. J., L. Zhang, J. L. Li, T. Xing, and F. Gao. 2022. Acute stress deteriorates breast meat quality of Ross 308 broiler chickens by inducing redox imbalance and mitochondrial dysfunction. J. Anim. Sci. 100:skac221.

Liu, B., D. Wang, E. Luo, J. Hou, Y. Qiao, G. Yan, Q. Wang, and C. Tang. 2020. Role of TG2-Mediated SERCA2 serotonylation on hypoxic pulmonary vein remodeling. Front. Pharmacol. 10:1611.

Lu, J., and A. Holmgren. 2014. The thioredoxin antioxidant system. Free Radic. Biol. Med. 66:75–87.

Maklad, A., A. Sharma, and I. Azimi. 2019. Calcium signaling in brain cancers: roles and therapeutic targeting. Cancers (Basel) 11:145.

Michelucci, A., C. Liang, F. Protasi, and R. T. Dirksen. 2021. Altered Ca2+ handling and oxidative stress underlie mitochondrial damage and skeletal muscle dysfunction in aging and disease. Metabolites 11:424.

Morad, M., Y. J. Suzuki, and E. Okabe. 2000. Redox regulation of cardiac and skeletal sarcoplasmic reticulum. Antioxid. Redox Signal. 2:1–3.

Mutryn, M. F., E. M. Brannick, W. Fu, W. R. Lee, and B. Abasht. 2015. Characterization of a novel chicken muscle disorder through differential gene expression and pathway analysis using RNA-sequencing. BMC Genomics 16:399.

Oberc, M. A., and W. K. Engel. 1977. Ultrastructural localization of calcium in normal and abnormal skeletal muscle. Lab. Invest. 36:566–577.

Pan, X. N., L. Zhang, T. Xing, J. L. Li, and F. Gao. 2021. The impaired redox status and activated nuclear factor-erythroid 2-related factor 2/antioxidant response element pathway in wooden breast myopathy in broiler chickens. Anim. Biosci. 34:652–661.

Papah, M. B., E. M. Brannick, C. J. Schmidt, and B. Abasht. 2017. Evidence and role of phlebitis and lipid infiltration in the onset and pathogenesis of Wooden Breast Disease in modern broiler chickens. Avian Pathol. 46:623–643.

Petracci, M., S. Mudalal, F. Soglia, and C. Cavani. 2015. Meat quality in fast-growing broiler chickens. World's Poult. Sci. J. 71:363–374.

Petracci, M., F. Soglia, M. Madruga, L. Carvalho, E. Ida, and M. Estévez. 2019. Wooden−breast, white striping, and spaghetti meat: causes, consequences and consumer perception of emerging broiler meat abnormalities. Compr. Rev. Food Sci. 18:565–583.

Polak, M., B. Przybylska-Gornowicz, and A. Faruga. 2009. Abnormal morphology of skeletal muscles in meat-type chickens: ultrastructural observations. Pol. J. Vet. Sci. 12:473–479.

Qualls, A. E., W. M. Southern, and J. A. Call. 2021. Mitochondria-cytokine crosstalk following skeletal muscle injury and disuse: a mini-review. Am. J. Physiol. Cell Physiol. 320:C681–C688.

Salles, G. B. C., M. M. Boiago, A. D. Silva, V. M. Morsch, A. Gris, R. E. Mendes, M. D. Baldissera, and A. S. da Silva. 2019. Lipid peroxidation and protein oxidation in broiler breast fillets with white striping myopathy. J. Food Biochem. 43:e12792.

Sevier, C. S., and C. A. Kaiser. 2008. Ero1 and redox homeostasis in the endoplasmic reticulum. Biochim. Biophys. Acta 1783:549–556.

Sihvo, H. K., K. mmonen, and E. Puolanne. 2014. Myodegeneration with fibrosis and regeneration in the pectoralis major muscle of broilers. Vet. Pathol. 51:619–623.

Strosova, M. K., J. Karlovska, P. Zizkova, M. Kwolek-Mirek, S. Ponist, C. M. Spickett, and L. Horakova. 2011. Modulation of sarcoplasmic/endoplasmic reticulum Ca(2+)-ATPase activity and oxidative modification during the development of adjuvant arthritis. Arch. Biochem. Biophys. 511:40–47.

Tang, X. Q., Y. X. Luo, H. Z. Chen, and D. P. Liu. 2014. Mitochondria, endothelial cell function, and vascular diseases. Front. Physiol. 5:175.

Taylor, C. W., and K. Machaca. 2019. IP3 receptors and store-operated Ca^{2+} entry: a license to fill. Curr. Opin. Cell Biol. 57:1–7.

Velleman, S. G. 2019. Recent developments in breast muscle myopathies associated with growth in poultry. Annu. Rev. Anim. Biosci. 7:289–308.

Velleman, S. G., and D. L. Clark. 2015. Histopathologic and myogenic gene expression changes associated with wooden breast in broiler breast muscles. Avian Dis. 59:410–418.

Velleman, S. G., D. L. Clark, and J. R. Tonniges. 2018. The effect of the wooden breast myopathy on sarcomere structure and organization. Avian Dis. 62:28–35.

Velleman, S. G., D. C. McFarland, Z. Li, N. H. Ferrin, R. Whitmoyer, and J. E. Dennis. 1997. Alterations in sarcomere structure, collagen organization, mitochondrial activity, and protein metabolism in the avian low score normal muscle weakness. Dev. Growth Differ. 39:563–570.

Wallace, D. C., and D. Chalkia. 2013. Mitochondrial DNA genetics and the heteroplasmy conundrum in evolution and disease. Cold. Spring Harb. Perspect. Biol. 5:a021220.

Wang, Z., E. Brannick, and B. Abasht. 2023. Integrative transcriptomic and metabolomic analysis reveals alterations in energy metabolism and mitochondrial functionality in broiler chickens with wooden breast. Sci. Rep 13:4747.

Wang, Y., R. Liu, X. Tian, X. Fan, Y. Shi, W. Zhang, Q. Hou, and G. Zhou. 2019. Comparison of activity, expression, and S-Nitrosylation of calcium transfer proteins between pale, soft, and exudative and red, firm, and non-exudative pork during post-mortem aging. J. Agric. Food Chem. 67:3242–3248.

Welter, A. A., W. J. Wu, R. Maurer, T. G. O'Quinn, M. D. Chao, D. L. Boyle, E. R. Geisbrecht, S. D. Hartson, B. C. Bowker, and H. Zhuang. 2022. An investigation of the altered textural property in woody breast myopathy using an integrative omics approach. Front. Physiol. 13:860868.

Xing, T., D. Luo, X. Zhao, X. L. Xu, J. L. Li, L. Zhang, and F. Gao. 2021. Enhanced cytokine expression and upregulation of inflammatory signaling pathways in broiler chickens affected by wooden breast myopathy. J. Sci. Food Agric. 101:279–286.

Xing, T., C. Wang, X. Zhao, C. Dai, G. H. Zhou, and X. L. Xu. 2017. Proteome analysis using isobaric tags for relative and absolute analysis quantitation (iTRAQ) reveals alterations in stress-induced dysfunctional chicken muscle. J. Agric. Food Chem. 65:2913–2922.

Zambonelli, P., M. Zappaterra, F. Soglia, M. Petracci, F. Sirri, C. Cavani, and R. Davoli. 2016. Detection of differentially expressed genes in broiler pectoralis major muscle affected by white striping−wooden breast myopathies. Poult. Sci. 95:1785–2771.

Zhang, W., S. Xiao, E. J. Lee, and D. U. Ahn. 2011. Consumption of oxidized oil increases oxidative stress in broilers and affects the quality of breast meat. J. Agric. Food Chem. 59:969–974.

Zhao, H., Y. Wang, Y. Shao, J. Liu, S. Wang, and M. Xing. 2018. Oxidative stress-induced skeletal muscle injury involves in NF-κB/p53-activated immunosuppression and apoptosis response in copper (II) or/and arsenite-exposed chicken. Chemosphere 210:76–84.

Zheng, S. Z., F. Yumei, and A. Chen. 2007. De novo synthesis of glutathione is a prerequisite for curcumin to inhibit hepatic stellate cell (HSC) activation. Free Radic. Biol. Med. 43:444–453.